

DOI:10.1002/ejic.201402099

Lanthanide Complexes Assembled from 3-Fluorophthalate and 1,10-Phenanthroline: Syntheses, Crystal Structure, Photoluminescence, and White-Light Emission

Yu-E Cha,^[a,bl] Xia Li,^{*[a]} Dou Ma,^[a] and Rui Huo^[a]

Keywords: Metal-organic frameworks / Luminescence / Lanthanides / Bridging ligands / Doping

Two different crystal forms, $[\text{Ln}_4(\text{Fpht})_6(\text{phen})_6(\text{H}_2\text{O})_4] \cdot n\text{H}_2\text{O}$ ($\text{Ln} = \text{Eu}$ **1**, $n = 14$; Tb **2**, $n = 12$) and $[\text{Ln}(\text{Fpht})(\text{HFpht})(\text{phen})(\text{H}_2\text{O})]$ ($\text{Ln} = \text{La}$ **3**, Eu **4**, Tb **5**) were obtained from the one-pot reaction of Ln^{III} ions with 3-fluorophthalic acid (H_2Fpht) and 1,10-phenanthroline (phen). Complexes **1** and **2** are centrosymmetric tetranuclear molecules with two crystallographically different Ln^{III} ion environments, $[\text{Ln}(1)\text{O}_6\text{N}_2]$ and $[\text{Ln}(2)\text{O}_4\text{N}_4]$. The complexes have a tridentate bridging Fpht ligand and a bidentate terminal Fpht ligand. Complexes **3–5**

show 2D networks with $[\text{LnO}_7\text{N}_2]$ polyhedra. There are two kinds of ligands, Fpht and HFpht , which adopt chelating-bridging/monodentate and bidentate-bridging coordination modes, respectively. The La^{III} complex shows ligand-centered fluorescence. Eu^{III} and Tb^{III} complexes display red $^5\text{D}_0 \rightarrow ^7\text{F}_{0-4}$ and green $^5\text{D}_4 \rightarrow ^7\text{F}_{6-2}$ characteristic luminescence, respectively. Intriguingly, white-light emission was produced when Eu^{III} and Tb^{III} were codoped into the 2D La^{III} complex.

Introduction

In the past two decades, metal-organic frameworks (MOFs) have received intense interest due to their novel architectures and potential applications as functional materials in fields such as gas storage, magnetism, catalysis, and sensors.^[1–4] Currently, there is increasing interest in white-light emitting materials based on MOFs.^[5–15] The interest in such materials stems from their promising applications in lighting light-emitting diodes and backlight sources.^[16–20] Lanthanide-containing MOFs (LnOFs) have received the most attention for constructing white-light emitting materials because they exhibit intense luminescence.^[5–13] Furthermore, it is possible to design isostructural compounds involving different lanthanide ions due to lanthanide contraction.

Red, green, and blue are the “primary” colors of white light and their combination can produce a white-light emission. Thus, Eu^{III} (red) and Tb^{III} (green) are promising candidates for white-light emitting materials based on the lanthanide complexes.^[5–11] It is important to design appropriate lanthanide complexes with chromophoric antenna ligands for efficient emission. In general, aromatic-conjugated systems have highly efficient light absorption and high efficiencies of intersystem crossing and energy transfer processes. Investigations have revealed that aromatic carb-

oxylates are sensitizing ligands for the emission of lanthanide complexes and they have been commonly used as linkers for the preparation of LnOFs that exhibit unique photophysical properties and intriguing structural features.^[21] It has also been well-documented that the π -conjugated 1,10-phenanthroline (phen) ligand is an efficient sensitizer for both Eu^{III} and Tb^{III} , and is usually inserted into lanthanide carboxylate complexes.^[10,22–24] 3-Fluorophthalic acid (H_2Fpht) is a suitable ligand for the preparation of luminescent lanthanide complexes.^[25] Because fluorinated organic ligands have low-vibrational frequency of C–F (1220 cm^{-1}), the luminescence intensity of complexes can be remarkably improved by reducing the fluorescence quenching effect of the vibrational C–H bond (the energy level C–H 2950 cm^{-1}).^[26–30] However, much less work has been carried out on coordination polymers of H_2Fpht .^[25,31,32] Therefore, the complexes $[\text{Ln}_4(\text{Fpht})_6(\text{phen})_6(\text{H}_2\text{O})_4] \cdot n\text{H}_2\text{O}$ ($\text{Ln} = \text{Eu}$ **1**, $n = 14$; Tb **2**, $n = 12$) and $[\text{Ln}(\text{Fpht})(\text{HFpht})(\text{phen})(\text{H}_2\text{O})]$ ($\text{Ln} = \text{La}$ **3**, Eu **4**, Tb **5**) were synthesized. Interestingly, **1** and **4**, and **2** and **5** were obtained from a one-pot reaction system, respectively. The complexes display different structural motifs: tetranuclear molecules (**1** and **2**) and 2D structures (**3** and **4**). The crystal structures and photophysical properties were investigated. Notably, through doping of the 2D frameworks, white-light emission was achieved when excited with a UV wavelength.

Results and Discussion

Description of the Structures

Complexes **1–2** and **3–5** are isostructural, respectively, hence, only the structures of **2** and **3** will be discussed in

[a] Beijing Key Laboratory for Optical Materials and Photonic Devices, Department of Chemistry, Capital Normal University, Beijing 100048, China
E-mail: xiali@mail.cnu.edu.cn
<http://www.cnu.edu.cn/>

[b] National Center for Rural Water Supply Technical Guidance, Chinese Center for Disease Control and Prevention, Beijing 102200, P. R. China

Supporting information for this article is available on the WWW under <http://dx.doi.org/10.1002/ejic.201402099>.

detail. A summary of the crystallographic data and details of the structure refinements are listed in Table 1. Selected bond lengths and bond angles are listed in Table S1.

The structure of **2** consists of a tetranuclear molecule $[\text{Tb}_4(\text{Fpht})_6(\text{phen})_6(\text{H}_2\text{O})_4]$ and crystallization water molecules. The $[\text{Tb}_4(\text{Fpht})_6(\text{phen})_6(\text{H}_2\text{O})_4]$ molecule has a tetranuclear centrosymmetry with two equivalent $\text{Tb}_2(\text{Fpht})_3(\text{phen})_3(\text{H}_2\text{O})_2$ moieties linked by two bridged COO groups of the two Fpht ligands (Figure 1, a). In each of two equivalent $\text{Tb}_2(\text{Fpht})_3(\text{phen})_3(\text{H}_2\text{O})_2$ moieties, two Tb^{III} (Tb(1) and Tb(2)) ions with different coordination environments are linked by one bridged COO group of the Fpht ligand. There are two crystallographically distinct Fpht ligands. The tridentate Fpht anions bridging ligand bridges two Tb^{III} ions through one unidentate carboxylate group and

one chelating-bridging carboxylate group (Scheme S1a). The bidentate Fpht anion as terminal ligand chelates with one Tb^{III} ion by two unidentate carboxylate oxygen atoms (Scheme S1b). Tb(1) is eight-coordinated by four O atoms from three Fpht ligands, two N atoms from one phen ligand, and two water molecules, whereas Tb(2) is eight-coordinated by four O atoms from two Fpht ligands, and four N atoms from two phen ligands. The phen ligand forms a five-membered chelate ring with each Tb^{III} ion by means of its two N atoms, where phen acts as terminal blocking ligand that prevents further polymerization because of the steric hindrance of the terminal ligands. The two terminal phen planes are ca. 78.38° apart. The distances of Tb1–O–(carboxyl), Tb1–O(water) and Tb1–N range from 2.307(3) to 2.367(3) Å, 2.430(4) to 2.435(4) Å, and 2.535(4) to

Table 1. Crystallographic data and structure refinement of complexes 1–5.

	1	2	3	4	5
Empirical formula	$\text{C}_{60}\text{H}_{49}\text{Eu}_2\text{F}_3\text{N}_6\text{O}_{21}$	$\text{C}_{60}\text{H}_{47}\text{F}_3\text{N}_6\text{O}_{20}\text{Tb}_2$	$\text{C}_{28}\text{H}_{17}\text{LaF}_2\text{N}_2\text{O}_9$	$\text{C}_{28}\text{H}_{17}\text{EuF}_2\text{N}_2\text{O}_9$	$\text{C}_{28}\text{H}_{17}\text{F}_2\text{N}_2\text{O}_9\text{Tb}$
Formula weight	1550.99	1546.88	702.35	715.40	722.36
<i>T</i> [K]	296(2)	296(2)	293(2)	298(2)	293(2)
Wavelength [Å]	0.71073	0.71073	0.71073	0.71073	0.71073
Crystal system	monoclinic	monoclinic	monoclinic	monoclinic	monoclinic
Space group	$P2_1/n$	$P2_1/n$	$P2_1/c$	$P2_1/c$	$P2_1/c$
<i>a</i> [Å]	11.8530(6)	11.8348(2)	12.6078(17)	12.9319(14)	12.541(3)
<i>b</i> [Å]	22.6293(10)	22.4499(3)	16.171(2)	16.4498(17)	15.909(4)
<i>c</i> [Å]	22.6381(11)	23.6199(3)	12.9635(18)	13.2232(15)	12.774(3)
β [°]	99.542(2)	109.7910(10)	102.747(2)	101.670(2)	101.462(4)
<i>V</i> [Å ³]	5988.1(5)	5904.90(15)	2577.8(6)	2754.8(5)	2497.7(10)
<i>Z</i>	4	4	4	4	4
<i>D</i> _{calcd.} [Mg m ⁻³]	1.713	1.740	1.810	1.725	1.921
<i>F</i> (000)	3060	3064	1384	1408	1416
Limiting indices	$-15 \leq h \leq 14,$ $-29 \leq k \leq 29,$ $-27 \leq l \leq 29$	$-15 \leq h \leq 15,$ $-29 \leq k \leq 29,$ $-30 \leq l \leq 31$	$-14 \leq h \leq 15,$ $-17 \leq k \leq 19,$ $-15 \leq l \leq 13$	$-15 \leq h \leq 14,$ $-19 \leq k \leq 19,$ $-7 \leq l \leq 15$	$-15 \leq h \leq 14,$ $-19 \leq k \leq 16,$ $-12 \leq l \leq 15$
Reflections collected/unique	14400/10410 [<i>R</i> (int) = 0.0368]	14107/9616 [<i>R</i> (int) = 0.0468]	12892/4667 [<i>R</i> (int) = 0.0338]	13510/4857 [<i>R</i> (int) = 0.1348]	11684/4509 [<i>R</i> (int) = 0.0395]
Data/restraints/parameters	14400/0/828	14107/0/820	4667/3/388	4857/0/379	4509/3/386
Goodness-of-fit on <i>F</i> ²	0.923	1.050	1.032	0.899	1.001
Final <i>R</i> indexes [<i>I</i> > 2σ(<i>I</i>)]	<i>R</i> ₁ = 0.0395, <i>wR</i> ₂ = 0.1177	<i>R</i> ₁ = 0.0417, <i>wR</i> ₂ = 0.1019	<i>R</i> ₁ = 0.0262, <i>wR</i> ₂ = 0.0597	<i>R</i> ₁ = 0.0550, <i>wR</i> ₂ = 0.0755	<i>R</i> ₁ = 0.0309, <i>wR</i> ₂ = 0.0685
<i>R</i> indexes [all data]	<i>R</i> ₁ = 0.0627, <i>wR</i> ₂ = 0.1390	<i>R</i> ₁ = 0.0714, <i>wR</i> ₂ = 0.1185	<i>R</i> ₁ = 0.0324, <i>wR</i> ₂ = 0.0625	<i>R</i> ₁ = 0.1194, <i>wR</i> ₂ = 0.0891	<i>R</i> ₁ = 0.0492, <i>wR</i> ₂ = 0.0771
Largest diff. peak and hole [e Å ⁻³]	0.887 and -0.791	0.823 and -1.363	0.473 and -0.468	1.561 and -1.046	1.027 and -1.008

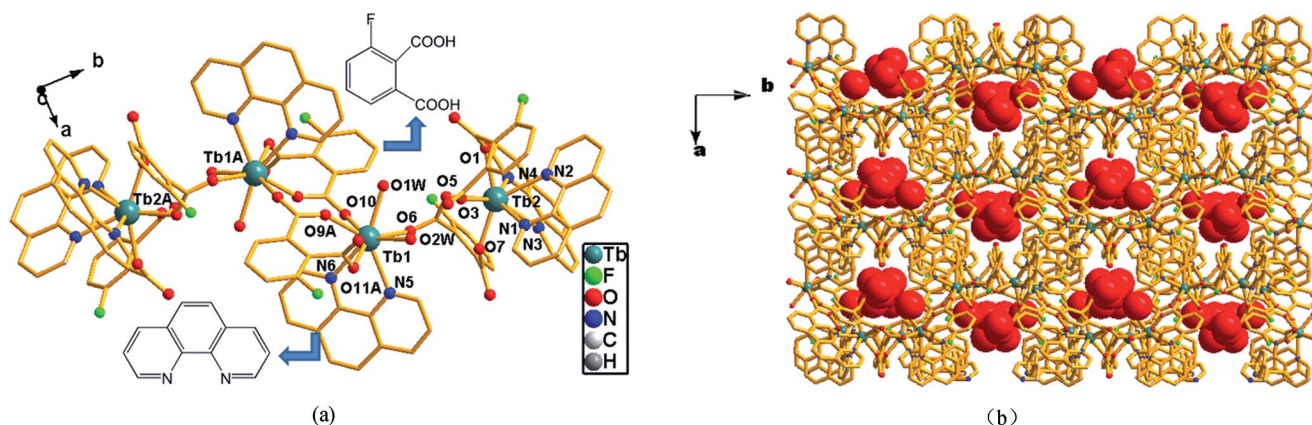


Figure 1. (a) Molecular structure of **2** and the structural formula of the ligands. All hydrogen atoms and uncoordinated water molecules are omitted for clarity; symmetry code: A: $-x, -y, -z$. (b) 3D supramolecular architecture.

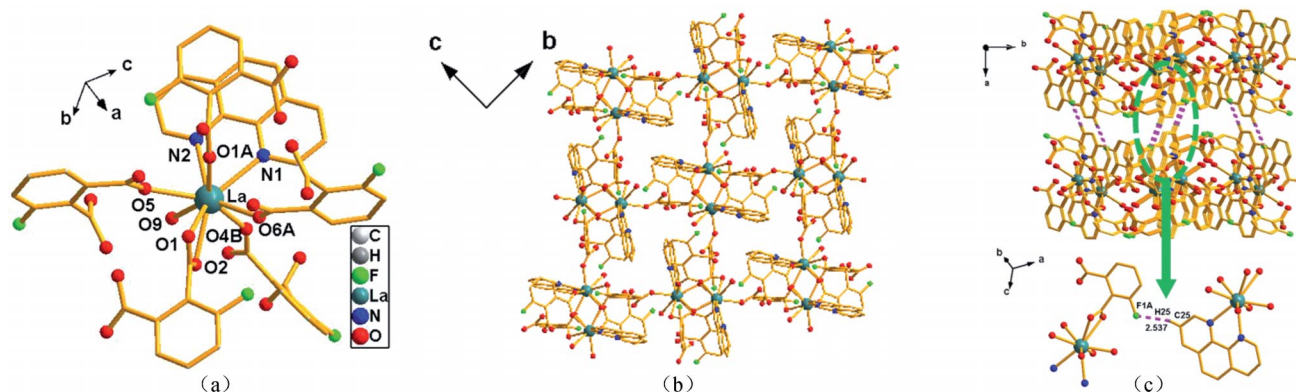


Figure 2. View of the structure of **3**. (a) The coordination environment of the La^{III} ion; free water molecules and H atoms are omitted for clarity; symmetry code: A: $-x + 1, -y, -z + 1$; B: $x, -y + 0.5, z + 0.5$. (b) 2D structure. (c) 3D supramolecular architecture and C–H...F hydrogen bonds; symmetry code: A: $x - 1, y, z$.

2.588(6) Å, respectively. The distances Tb2–O(carboxyl) and Tb2–N range from 2.289(4) to 2.395(3) Å, and 2.527(4) to 2.605(4) Å, respectively. Tb1 and Tb1A ions are interconnected by two COO groups from two tridentate Fpht anions, whereas Tb2 and Tb1, and Tb1A and Tb2A are together linked by one COO group from one tridentate Fpht anion, respectively, to form a tetranuclear molecule. For the tetranuclear Tb(2)···Tb(1)···Tb(1A)···Tb(2A), the distance Tb(1)···Tb(1A) of 5.751(2) Å is slightly shorter than that of Tb(1)···Tb(2) [or Tb(1A)···Tb(2A)], which is 5.822(2) Å. The four Tb^{III} ions are strictly coplanar. The tetranuclear molecules are linked together by hydrogen bonds involving lattice water, coordination water, and carboxylate oxygen atoms, giving rise to a 3D array (Figure 1, b; Table S2). The crystallization water molecules are tightly H-bonded to the tetranuclear molecule in the crystal packing. The observed distances of Ln–O, Ln–N, and Ln···Ln in **1** and **2** decrease from Eu to Tb, respectively. Tetranuclear Ln^{III} complexes are very rare and, to the best of our knowledge, only two examples of such complexes have been reported.^[33,34]

Structure of [Ln(Fpht)(HFpht)(phen)(H₂O)] (Ln = La **3**, Eu **4**, Tb **5**)

The crystal structures of complexes **3–5** consist of 2D polymeric networks. The asymmetric unit of **3** comprises one La^{III} ion, one Fpht, one HFpht, one phen, and one water molecule. There is only one La^{III} environment in **3**, as shown in Figure 2 (a). Each La^{III} ion is bound to four O atoms from three Fpht anions, two O atoms from two HFpht anions, one water molecule, and two N atoms from a chelating phen molecule, thus resulting in a nine-coordinate environment. The distances of La–O(carboxyl) range from 2.415(2) to 2.799(2) Å and those of La–N are 2.714(3) and 2.735(3) Å. The distance of La–O(water) is 2.611(2) Å. The Ln–O and Ln–N distances are similar to those found in complexes **1–2**. There are two kinds of anions, Fpht and HFpht. The Fpht ligand adopts a chelating-bridging/monodentate coordination mode (Scheme S1, c). One carboxylate group of HFpht ligand adopts a bidentate-bridging coordination mode and the protonated carboxylate group remains

uncoordinated (Scheme S1d). The carboxylate groups of Fpht and HFpht are twisted relative to their respective aromatic ring planes by 38.3°/86.6° and 33.1°/80.4°, respectively. The adjacent La^{III} ions are bridged by two chelating-bridging carboxylate groups from two Fpht anions and two bidentate-bridging carboxylate groups from two HFpht anions to afford the [La₂(COO)₄] dimeric units with a La···La distance of 4.198 Å. The [La₂(COO)₄] unit can be viewed as a basic building block for the whole structure; such blocks are connected through Fpht ligands in two different directions, giving rise to a layer structure with a La···La distance of 8.602 Å (Figure 2, b). The [La₂(COO)₄] unit can be viewed as four-connected nodes, and then the layer can be simplified as a (4,4) net with the Schläfli symbol of (4⁴). A 3D supramolecular architecture is formed through hydrogen bonds between the C–H portions of the phen ligand and the F atoms of Fpht ligands from neighboring layers, C25–H25···F1A [H25···F1 2.537 Å, C12···F1 3.428 Å, C12–H12···F1, 160.31°] (Figure 2, c).

A comparison of the average Ln–O, Ln–N, and Ln···Ln distances for complexes **3**, **4** and **5**, reveals that the corresponding distances decrease in the order La^{III} > Eu^{III} > Tb^{III}, respectively, which is in agreement with the lanthanide contraction along the row of trivalent lanthanide ions.

Thermogravimetric Analysis (TGA)

The thermal stabilities of all complexes were explored by means of TGA in the temperature range from room temperature to 800 °C. The TGA curves of **1** and **2** exhibit similar features (Figure 3). The first weight loss of 7.77% for **1** and 7.99% for **2** occurs in the range of 38–148 °C for **1** and 35–155 °C for **2**, which is equivalent to the release of free water molecules (calcd. 8.12% for **1** and 7.09% for **2**). The anhydrous compounds decompose up to 250 °C for **1** and 257 °C for **2**, and completely decompose at 517 °C for **1** and 546 °C for **2**. The complexes **2–4** do not contain guest molecules, the TGA curve presents thermal stability up to 254 °C for **3**, 258 °C for **4** and 269 °C for **5**, at which point the complexes begin decomposition with mass loss corre-

sponding to the organic ligands; this process persists up to 525 °C for **3**, 515 °C for **4**, and 574 °C for **5**. The remaining weight corresponds to the formation of lanthanide oxide (observed: 23.96% for **1**, 26.68% for **2**, 26.41% for **3**, 27.59% for **4** and 29.10% for **5**; calculated: 21.91% for **1**, 24.62% for **2**, 23.26% for **3**, 24.60% for **4** and 26.42% for **5**).

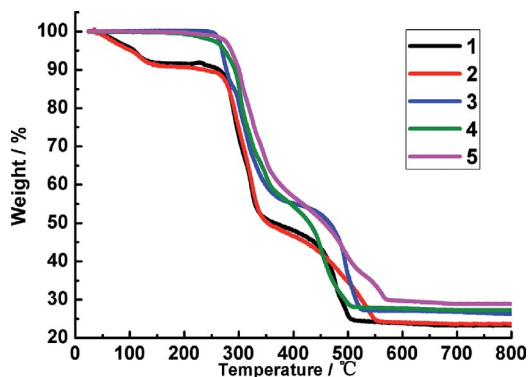


Figure 3. The TGA curves of **1**–**5**.

Luminescent Properties

Photoluminescence measurements of the ligands and complexes were acquired at room temperature. Under excitation at 377 nm, the ligands display broad emission bands centered at 439 nm for H₂Fpht and 436 nm for phen, which can be attributed to intraligand $\pi^*-\pi$ transition. Under excitation at 400 nm, complex **3** presents a blue emission band centered at 432 nm, which is similar to fluorescence of the free ligands. An enhancement in the intensity is observed compared with that of the free ligands (Figure 4). The luminescence lifetime value is 0.011 ms (Figure S1). Thus, we assume that the emission may be attributed to the fluorescence of ligands. This is in accordance with the fact that there is no f–f transition for the La^{III} ion. The excitation spectra were recorded in the range from 200 to 400 nm with a wavelength monitored for the Eu^{III} $^5D_0 \rightarrow ^7F_2$ transition (613 nm) of **4** and the Tb^{III} $^5D_4 \rightarrow ^7F_5$ transition (544 nm)

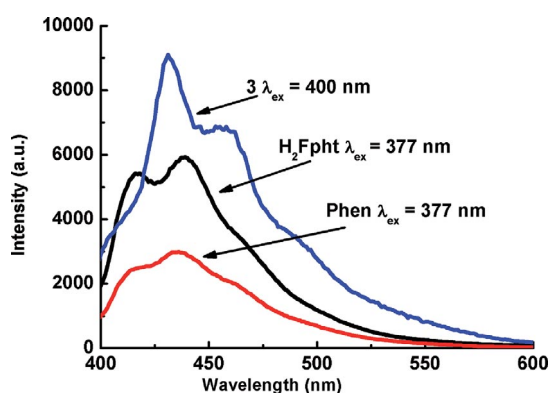


Figure 4. Emission spectra of H₂Fpht, phen and complex **3** in the solid state at room temperature.

of **5** (Figure 5). The excitation spectra exhibit large broad bands centered at 350 nm ascribed to the organic ligand and narrow bands at 394 nm attributed to the transition $^7F_0 \rightarrow ^5L_6$ for the Eu^{III} ion in **4** and at 379 nm for the $^7F_6 \rightarrow ^5D_3$ transition of the Tb^{III} ion in **5**. However, the narrow bands are weaker than the absorption of the organic ligand, which proves that luminescence sensitization through excitation of the ligand is much more efficient than direct excitation of the Eu^{III} or Tb^{III} ions absorption levels. The emission spectra of **4** and **5** were recorded under the maximum excitation wavelength at 350 nm. The emission spectrum of **4** is composed of the first excited state, 5D_0 , and the ground septet, 7F_J ($J = 0-4$) of Eu^{III} (Figure 6, a). The hypersensitive transition $^5D_0 \rightarrow ^7F_2$ splits into two peaks at 613 and 617 nm and is the strongest emission, resulting in red fluorescence. The magnetic transition $^5D_0 \rightarrow ^7F_1$ centers at 590 nm and is relatively weak. The intensity ratio of 1.47 for $I(^5D_0 \rightarrow ^7F_2)/I(^5D_0 \rightarrow ^7F_1)$ indicates a low symmetry of the Eu^{III} site in **4**. The very weak peaks at 579, 650 and 698 nm correspond to the transitions $^5D_0 \rightarrow ^7F_0$, $^5D_0 \rightarrow ^7F_3$, and $^5D_0 \rightarrow ^7F_4$, respectively. Complex **5** shows emission bands at 488, 543, 586, and 618 nm, which correspond to the characteristic transitions $^5D_4 \rightarrow ^7F_J$ ($J = 6-3$) of the Tb^{III} ion (Figure 6, b). The most intense emission at 543 nm, corresponding to the $^5D_4 \rightarrow ^7F_5$ transition, results in green fluorescence. For **4** and **5**, the absence of emission from the ligand triplet states points out the presence of an efficient ligand-to-Eu^{III}/Tb^{III} ions energy-transfer mechanism, which demonstrates that the ligands are suitable for sensitizing the Eu^{III}/Tb^{III} luminescence. In addition, complexes **4** and **5** were also investigated by exciting at f–f absorption of the Eu^{III} and Tb^{III} ions, respectively. At excitation wavelength 394 nm for **4** and 379 nm for **5**, the emission intensity of the $^5D_0 \rightarrow ^7F_J$ ($J = 0-4$) transitions for **4** and $^5D_4 \rightarrow ^7F_J$ ($J = 6-3$) transitions for **5** is lower than that at the ligand excitation maxima (350 nm). This indicates that ligand-to-Ln^{III} energy transfer is effective in **4** and **5**. The complex **4** has a luminescent quantum yield of 12.2% and a lifetime value of 0.595 ms, whereas complex **5** exhibits a higher quantum yield of 60.29% and longer a lifetime of 1.041 ms, indicating the superior match of the triplet energy level of ligands to that of the Tb^{III} emitting level. Because the lowest emitting level (around 20,

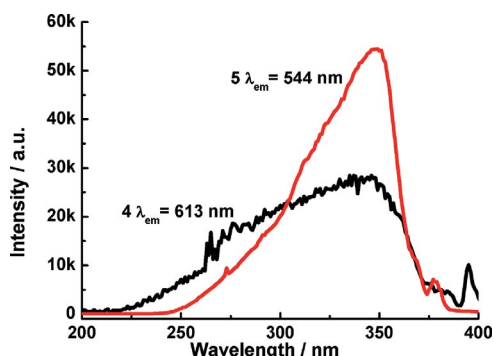


Figure 5. Excitation spectra of **4** and **5** in the solid state at room temperature.

500 cm^{-1}) of Tb^{III} is higher than that (around 17, 500 cm^{-1}) of Eu^{III} ion, the energy transfer from the ligand to the Tb^{III} ion is more efficient than that to the Eu^{III} ion. The observed luminescence decay profiles (Figure 6, inset) correspond to single exponential functions, thus implying the presence of only one emissive Eu^{III} or Tb^{III} center. The photoluminescence spectra of complexes **1** and **2** show similar characteristic emissions to those of the corresponding Eu^{III} ion in **4** and Tb^{III} ion in **5**, respectively (Figure S2).

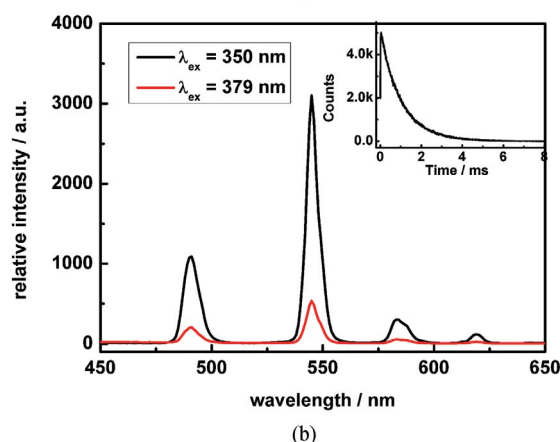
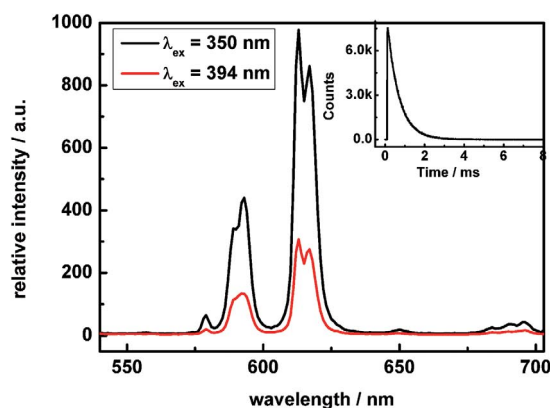


Figure 6. Emission spectra of **4** (a) and **5** (b) in the solid state at room temperature. Inset: decay profile of the complexes.

Considering that complexes **3**, **4**, and **5** emit the primary colors (blue, red, and green), it is therefore possible to construct white-light MOFs through doping of Eu^{III} and Tb^{III} into the La^{III} complex. Thus, the $\text{La}_{18}\text{Eu}_2\text{Tb}_{80}$ -doped material was produced and its phase purity was verified by powder X-ray diffraction (PXRD) analysis (Figure S3). The emission spectrum of the $\text{La}_{18}\text{Eu}_2\text{Tb}_{80}$ -doped material is composed of a broad band and a series of sharp lines (Figure 7). The broad emission band between 400 and 470 nm is ascribed to the ligands in **3**. The narrow emission bands at 492 and 546 nm, and at 590 and 613 nm arise from the characteristic transitions of Tb^{III} and Eu^{III} ion, respectively. The bands at 586 and 618 nm of the Tb^{III} ion overlap with the bands at 590 and 613 nm of the Eu^{III} ion. Upon excitation from 370 to 375 nm, the Commission International de l'Éclairage (CIE) chromaticity coordinates (Table S3)

change from (x, y) A (0.329, 0.336) to B (0.273, 0.253) falling within the white light region. The coordinate A (0.329, 0.336) excited at 370 nm is very close to the standard white light (0.333, 0.333) according to 1931 CIE coordinate diagram.^[35] The color rendering index (CRI) and correlated color temperature (CCT) are 88 and 5658 K, respectively. CRI values up to 80 correspond to a warm-white light that is appropriate for solid-state light applications. However, the CIE coordinates change from C (0.377, 0.395) to D (0.433, 0.480) with a decrease in the excitation wavelength from 365 to 350 nm, falling within the yellow-light region, whereas the CIE coordinates change from E (0.241, 0.208) to F (0.192, 0.135) with an increase in the excitation wavelength from 380 to 390 nm, falling within the blue-light region (Figure 8). Therefore, the doped material provides a promising and convenient approach to obtain uniform white light emitting or tunable luminescent MOFs. Because simultaneous luminescence of Tb^{III} and Eu^{III} occurs in the La^{III} complex to give green and red emission under UV excitation, this system therefore provides an approach with which to explore tunable white-light luminescence of LnOFs.

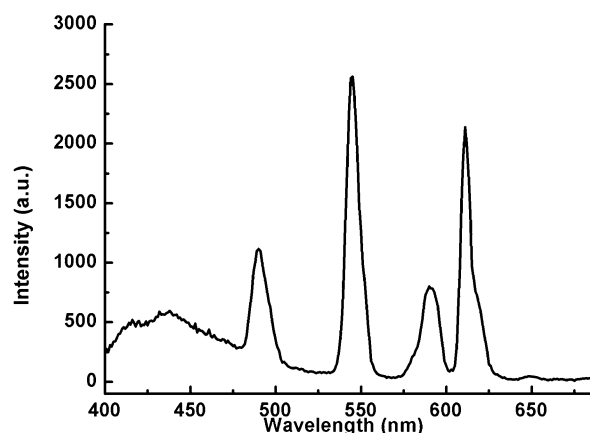


Figure 7. Emission spectra of the $\text{La}_{18}\text{Eu}_2\text{Tb}_{80}$ -doped material excited at 370 nm.

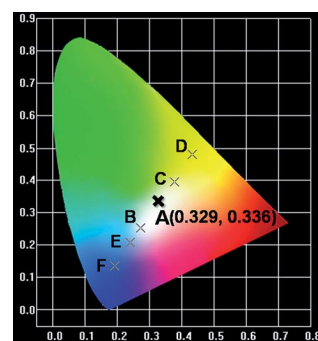


Figure 8. The CIE chromaticity diagram of the $\text{La}_{18}\text{Eu}_2\text{Tb}_{80}$ -doped material excited at 370 nm (A), 375 nm (B), 350 nm (D), 365 nm (C), 380 nm (E), and 390 nm (F).

Conclusions

Tetranuclear molecules $[\text{Ln}_4(\text{Fpht})_6(\text{phen})_6(\text{H}_2\text{O})_4] \cdot n\text{H}_2\text{O}$ ($\text{Ln} = \text{Eu}$ **1**, Tb **2**) and 2D frameworks $[\text{Ln}(\text{Fpht})(\text{HFpht})(\text{phen})(\text{H}_2\text{O})]$ ($\text{Ln} = \text{La}$ **3**, Eu **4**, Tb **5**) were synthesized in a one-pot reaction system. The two types of complexes show different thermal stabilities and luminescence properties because they involve different Ln^{III} coordination geometry. The La^{III} complex shows ligand-centered luminescence in the blue light. The Eu^{III} - and Tb^{III} -containing complexes exhibit typical intra-4f narrow line-emission in red and green light, respectively. Complexes **4** and **5** exhibit high quantum yield and longer lifetime and can be good candidates for light-emitting applications. In particular, Tb -containing complex **5** has a high quantum yield of 60%. The combination of La^{III} , Eu^{III} , and Tb^{III} ions for isomorphous 2D complexes **3–5** allows fine-tuning of the photoluminescence by changing the excitation wavelength, and the emission can be tuned from yellow to white. Finally, white-light emission was successfully realized. The different compositions of $\text{La}/\text{Eu}/\text{Tb}$ -doped complexes can be used for tunable and white-light emitting materials, which have potential applications in the fields of labeling, sensing, and color displays.

Experimental Section

Experimental Details and Physical Measurements: All reagents were commercially available and were used without further purification. Elemental analyses (C, H, and N) were determined with an Elementar Vario EL analyzer. IR spectra were recorded with a Nicolet Magna 750 FT/IR spectrometer using the KBr pellet technique in the range of 400–4000 cm^{-1} . X-ray diffraction was performed with a PANalytical X'Pert PRO MPD diffractometer for $\text{Cu-K}\alpha$ radiation ($\lambda = 1.5406 \text{ \AA}$), with a scan speed of 2°min^{-1} and a step size of 0.02° in 2θ . The simulated PXRD patterns were obtained from the single-crystal X-ray diffraction data. The experimental PXRD patterns are identical with the calculated spectra obtained from the single-crystal structures, confirming the phase purity of the bulk samples. The fluorescence spectra were recorded with an FL4500 fluorescence spectrophotometer (Japan Hitachi company) at room temperature. The lifetimes were measured at room temperature with a Life Spec-Red Picosecond lifetime spectrometer (Edinburgh Instruments). The emission quantum yields were measured at room temperature by using a quantum yield measurement system (Fluorolog-3; HORIBA company) with a 450 W Xe lamp coupled to a monochromator for wavelength discrimination, an integrating sphere as sample chamber, and an analyzer R928P for signal detection. The CIE color coordinates were calculated based on international CIE standards.^[35] Thermogravimetric analyses (TGA) were carried out with a Shimadzu DTG-60AH thermal analyzer (Japan) under air from room temperature to 800 $^\circ\text{C}$ with a heating rate of 10 $^\circ\text{C}/\text{min}$.

Synthesis of Complexes: Preparation of $[\text{Ln}_4(\text{Fpht})_6(\text{phen})_6(\text{H}_2\text{O})_4] \cdot n\text{H}_2\text{O}$ ($\text{Ln} = \text{Eu}$ **1**, $n = 14$; Tb **2**, $n = 12$) and $[\text{Ln}(\text{Fpht})(\text{HFpht})(\text{phen})(\text{H}_2\text{O})]$ ($\text{Ln} = \text{La}$ **3**, Eu **4**, Tb **5**): A mixture of $\text{Ln}(\text{NO}_3)_3 \cdot 6\text{H}_2\text{O}$ ($\text{Ln} = \text{La}$, Eu , Tb) (0.1 mmol), 3-fluorophthalic acid (0.2 mmol), phen (0.2 mmol), H_2O (8.0 mL), $\text{C}_2\text{H}_5\text{OH}$ (2.0 mL), and 2 mol/L NaOH (2 mL) was sealed in a 25 mL stainless-steel reactor with Teflon liner and heated to 170 $^\circ\text{C}$. The system was

then cooled to room temperature and colorless crystals of **3**, **4** and **5** were collected. The resulting solution was filtered and the filtrate was allowed to stand at room temperature without further disturbance for two weeks to give colorless crystals of **1** and **2**.

Complex 1: Yield 20% based on Eu^{III} . $\text{C}_{120}\text{H}_{98}\text{Eu}_4\text{F}_6\text{N}_{12}\text{O}_{40}$ (3069.98): calcd. C 46.40, H 3.18, N 5.40; found C 46.69, H 2.98, N 5.50. IR (KBr pellet): $\tilde{\nu} = 3411$ (s, br), 1600 (s), 1563 (s), 1519 (m), 1463 (m), 1424 (m), 1399 (s), 1382 (s), 1240 (m), 847 (m), 772 (m), 730 (m), 465 (w) cm^{-1} .

Complex 2: Yield 20% based on Tb^{III} . $\text{C}_{120}\text{H}_{94}\text{F}_6\text{N}_{12}\text{O}_{40}\text{Tb}_4$ (3093.81): calcd. C 46.59, H 3.06, N 5.40; found C 46.74, H 3.28, N 5.39. IR (KBr pellet): $\tilde{\nu} = 3410$ (s, br), 1601 (s), 1563 (s), 1518 (m), 1463 (m), 1424 (m), 1400 (s), 1381 (s), 1240 (m), 847 (m), 772 (m), 730 (m), 464 (w) cm^{-1} .

Complex 3: Yield 49% based on La^{III} . $\text{C}_{28}\text{H}_{15}\text{F}_2\text{LaN}_2\text{O}_9$ (700.34): calcd. C 48.02, H 2.16, N 4.00; found C 48.07, H 2.20, N 3.95. IR (KBr pellet): $\tilde{\nu} = 3430$ (m, br), 1733 (m), 1626 (s), 1602 (s), 1546 (s), 1519 (m), 1476 (m), 1454 (m), 1402 (s), 1251 (m), 962 (m), 862 (m), 779 (m), 725 (m), 677 (w), 581 (w), 463 (w) cm^{-1} .

Complex 4: Yield 43% based on Eu^{III} . $\text{C}_{28}\text{H}_{17}\text{EuF}_2\text{N}_2\text{O}_9$ (715.41): calcd. C 47.00, H 2.40, N 3.92; found C 46.86, H 2.28, N 3.66. IR (KBr pellet): $\tilde{\nu} = 3540$ (m, br), 1734 (m), 1636 (s), 1605 (s), 1547 (s), 1519 (m), 1478 (m), 1455 (m), 1398 (s), 1250 (m), 962 (m), 863 (m), 781 (m), 724 (m), 677 (w), 584 (w), 464 (w) cm^{-1} .

Complex 5: Yield 48% based on Tb^{III} . $\text{C}_{28}\text{H}_{17}\text{F}_2\text{N}_2\text{O}_9\text{Tb}$ (722.37): calcd. C 46.56, H 2.37, N 3.88; found C 46.32, H 2.24, N 3.96. IR (KBr pellet): $\tilde{\nu} = 3434$ (m, br), 1734 (m), 1624 (s), 1606 (s), 1546 (s), 1519 (m), 1480 (m), 1453 (m), 1405 (s), 1248 (m), 963 (m), 863 (m), 781 (m), 725 (m), 695 (w), 584 (w), 465 (w) cm^{-1} .

$\text{La}_{18}\text{Eu}_2\text{Tb}_{80}$ Doped Complex: Anal. Calc. for $\text{La}_{18}\text{Eu}_2\text{Tb}_{80}$ -doped complex: C, 47.25; H, 2.20, N, 4.09%. IR (KBr pellet): $\tilde{\nu} = 3426$ (m, br), 1734 (m), 1625 (s), 1602 (s), 1576 (s), 1545 (s), 1519 (m), 1477 (m), 1456 (m), 1400 (s), 1241 (m), 962 (m), 862 (m), 779 (m), 727 (m), 695 (w), 581 (w), 483 (w) cm^{-1} .

X-ray Crystallography Study: The X-ray single-crystal data collections for the five complexes were performed with a Bruker SMART CCD diffractometer using graphite monochromatized $\text{Mo-K}\alpha$ radiation ($\lambda = 0.71073 \text{ \AA}$). Semiempirical absorption corrections were applied. The structures were solved by direct methods and refined by full-matrix least-squares method on F^2 using the SHELXS-97 and SHELXL-97 programs.^[36,37] All non-hydrogen atoms in the complexes were refined anisotropically. The hydrogen atoms were generated geometrically and treated by a mixture of independent and constrained refinement. A summary of the crystallographic data and details of the structure refinements is listed in Table 1. Selected bond lengths and bond angles are listed in Table S1.

CCDC-917459 (for **1**), -917460 (for **2**), -917462 (for **3**), -917463 (for **4**), and -917464 (for **5**) contain the supplementary crystallographic data for this paper. These data can be obtained free of charge from The Cambridge Crystallographic Data Centre via www.ccdc.cam.ac.uk/data_request/cif.

Supporting Information (see footnote on the first page of this article): X-ray crystallographic files in CIF format, selected bond lengths and bond angles (Tables S1) and H-bonds for **2** (Tables S2). The PXRD patterns for complexes and the codoped complex (Figure S1). The coordination modes of Fpht and HFpht ligands (Scheme S1). Emission spectra of complexes **1(a)** and **2 (b)** in the solid state at room temperature (Figure S3). CIE chromaticity coordinates for the codoped complexes (Table S3).

Acknowledgments

The authors are grateful to the National Natural Science Foundation of China (NSFC) (grant number 21071101) and the Beijing Municipal Science & Technology Commission (grant number Z131103002813097).

- [1] S. Kitagawa, R. Kitaura, S.-i. Noro, *Angew. Chem. Int. Ed.* **2004**, *43*, 2334–2375; *Angew. Chem.* **2004**, *116*, 2388.
- [2] E. Coronado, G. M. Espallargas, *Chem. Soc. Rev.* **2013**, *42*, 1525–1539.
- [3] J. Lee, O. K. Farha, J. Roberts, K. A. Scheidt, S. T. Nguyen, J. T. Hupp, *Chem. Soc. Rev.* **2009**, *38*, 1450–1459.
- [4] L. E. Kreno, K. Leong, O. K. Farha, M. Allendorf, R. P. Van Duyne, J. T. Hupp, *Chem. Rev. (Washington, DC, U. S.)* **2011**, *112*, 1105–1125.
- [5] L. D. Carlos, R. A. Ferreira, V. d. Z. Bermudez, S. J. Ribeiro, *Adv. Mater.* **2009**, *21*, 509–534.
- [6] P. Falcaro, S. Furukawa, *Angew. Chem. Int. Ed.* **2012**, *51*, 8431–8433; *Angew. Chem.* **2012**, *124*, 8557.
- [7] H. Zhang, X. Shan, L. Zhou, P. Lin, R. Li, E. Ma, X. Guo, S. Du, *J. Mater. Chem.* **2013**, *1*, 888–891.
- [8] S. Dang, J.-H. Zhang, Z.-M. Sun, *J. Mater. Chem.* **2012**, *22*, 8868–8873.
- [9] X. Rao, Q. Huang, X. Yang, Y. Cui, Y. Yang, C. Wu, B. Chen, G. Qian, *J. Mater. Chem.* **2012**, *22*, 3210–3214.
- [10] X. Ma, X. Li, Y.-E. Cha, L.-P. Jin, *Cryst. Growth Des.* **2012**, *12*, 5227–5232.
- [11] S.-L. Zhong, R. Xu, L.-F. Zhang, W.-G. Qu, G.-Q. Gao, X.-L. Wu, A.-W. Xu, *J. Mater. Chem.* **2011**, *21*, 16574–16580.
- [12] S. Song, X. Li, Y.-H. Zhang, R. Huo, D. Ma, *Dalton Trans.* **2014**, *43*, 5974–5977.
- [13] Y.-H. Zhang, X. Li, S. Song, *Chem. Commun.* **2013**, *49*, 10397–10399.
- [14] D. F. Sava, L. E. Rohwer, M. A. Rodriguez, T. M. Nenoff, *J. Am. Chem. Soc.* **2012**, *134*, 3983–3986.
- [15] F. Luo, M.-S. Wang, M.-B. Luo, G.-M. Sun, Y.-M. Song, P.-X. Li, G.-C. Guo, *Chem. Commun.* **2012**, *48*, 5989–5991.
- [16] E. F. Schubert, J. K. Kim, *Science* **2005**, *308*, 1274–1278.
- [17] C. Feldmann, T. Jüstel, C. R. Ronda, P. J. Schmidt, *Adv. Funct. Mater.* **2003**, *13*, 511–516.
- [18] H. A. Höppe, *Angew. Chem. Int. Ed.* **2009**, *48*, 3572–3582; *Angew. Chem.* **2009**, *121*, 3626.
- [19] E. Downing, L. Hesselink, J. Ralston, R. Macfarlane, *Science* **1996**, *273*, 1185–1188.
- [20] T. Jüstel, H. Nikol, C. Ronda, *Angew. Chem. Int. Ed.* **1998**, *37*, 3084–3103; *Angew. Chem.* **1998**, *110*, 3250.
- [21] M. Allendorf, C. Bauer, R. Bhakta, R. Houk, *Chem. Soc. Rev.* **2009**, *38*, 1330–1352.
- [22] Y.-B. Wang, X.-J. Zheng, W.-J. Zhuang, L.-P. Jin, *Eur. J. Inorg. Chem.* **2003**, 3572–3582.
- [23] Y.-X. Chi, S.-Y. Niu, Z.-L. Wang, J. Jin, *Eur. J. Inorg. Chem.* **2008**, 2336–2343.
- [24] Y. Li, F.-K. Zheng, X. Liu, W.-Q. Zou, G.-C. Guo, C.-Z. Lu, J.-S. Huang, *Inorg. Chem. (Washington, DC, U. S.)* **2006**, *45*, 6308–6316.
- [25] Y.-E. Cha, X. Li, S. Song, *J. Solid State Chem.* **2012**, *196*, 40–44.
- [26] M. Irfanullah, K. Iftikhar, *J. Fluoresc.* **2011**, *21*, 81–93.
- [27] Y. Wada, T. Okubo, M. Ryo, T. Nakazawa, Y. Hasegawa, S. Yanagida, *J. Am. Chem. Soc.* **2000**, *122*, 8583–8584.
- [28] B.-L. Chen, Y. Yang, F. Zapata, G.-D. Qian, Y.-S. Luo, J.-H. Zhang, E. B. Lobkovsky, *Inorg. Chem. (Washington, DC, U. S.)* **2006**, *45*, 8882–8886.
- [29] G. Mancino, A. J. Ferguson, A. Beeby, N. J. Long, T. S. Jones, *J. Am. Chem. Soc.* **2005**, *127*, 524–525.
- [30] D. A. Raj, B. Francis, M. Reddy, R. R. Butorac, V. M. Lynch, A. H. Cowley, *Inorg. Chem. (Washington, DC, U. S.)* **2010**, *49*, 9055–9063.
- [31] Y.-E. Cha, X. Li, X. Ma, C.-Q. Wan, X.-B. Deng, L.-P. Jin, *CrystEngComm* **2012**, *14*, 5322–5329.
- [32] Y.-E. Cha, X. Ma, X. Li, H.-Z. Shi, H.-L. Tan, Y. Meng, *Inorg. Chem. Commun.* **2012**, *20*, 108–111.
- [33] X. Li, C.-Y. Wang, H.-M. Hu, *Inorg. Chem. Commun.* **2008**, *11*, 345–348.
- [34] C.-Q. Wan, X. Li, C.-Y. Wang, X. Qiu, *J. Mol. Struct.* **2009**, *930*, 32–36.
- [35] T. Smith, J. Guild, *J. Trans. Opt. Soc.* **1931**, *33*, 73.
- [36] G. M. Sheldrick, *SHELXTL*, v. 5.1, Bruker Analytical X-ray Instruments Inc., Madison, Wisconsin, USA, **1998**.
- [37] G. M. Sheldrick, *SHELX-97*, PC version, University of Göttingen, Germany, **1997**.

Received: February 24, 2014
Published Online: May 27, 2014